Am J Transl Res 2025;17(1):60-74
www.ajtr.org /ISSN:1943-8141/AJTR0158237

*Original Article*

# Hepatoprotective effect of *Jasminum sambac* decoction against paracetamol-induced toxicity: *in silico*, *in vitro* and *in vivo* studies

Imran Ahmad Khan[1], Abdul Malik[2], Muhammad Omer Iqbal[3], Maliha Khalid Khan[4,5], Qurat ul Ain[4,5], Perwasha Perwasha[5], Asma Shahrukh[6], Sabiha Fatima[7]

*[1]Department of Pharmacy, MNS University of Agriculture, Multan 60000, Punjab, Pakistan; [2]Department of Pharmaceutics, College of Pharmacy, King Saud University, Riyadh 11495, Saudi Arabia; [3]Key Laboratory of Marine Drugs, The Ministry of Education, School of Medicine and Pharmacy, Ocean University of China, Qingdao 266003, Shandong, China; [4]Department of Pathobiology and Biomedical Sciences, MNS University of Agriculture, Multan 60000, Punjab, Pakistan; [5]Ali-Ul-Murtaza Department of Rehabilitation Sciences, Muhammad Institute of Medical and Allied Sciences, Multan 60000, Punjab, Pakistan; [6]College of Pharmacy, The University of Punjab, Lahore, Punjab, Pakistan; [7]Department of Clinical Laboratory Science, College of Applied Medical Sciences, King Saud University, Riyad, Saudi Arabia*

Received June 3, 2024; Accepted October 30, 2024; Epub January 15, 2025; Published January 30, 2025

**Abstract:** Objective: We aimed to investigate the pharmacologic mechanism underlying this traditional remedy. Method: We used a freshly produced hot water decoction of *J. sambac* leaves (HWDJS) to examine its hepatoprotective effects in laboratory animals, administering doses of HWDJS at 100, 200, and 300 mg/kg over 7 days. On the 8th day, paracetamol toxicity was induced at a dose of 2 g/kg. The test and control groups assessed biochemical indicators (alkaline phosphatase, aspartate transaminase, alanine transaminase, and C-reactive protein), liver-to-body weight ratio, and cytoarchitecture. Oxidative biomarkers (gamma-glutamyl-glycine, superoxide dismutases, and malondialdehyde) were measured after 24 hours of toxicity induction to judge the extent of hepatoprotection. Result: HWDJS confirmed a significant ($P \leq 0.05$) decrease in biochemical markers compared to the intoxicated group: histopathologic differences and antioxidant measures. The antioxidant potential of HWDJS was confirmed by a 2,2-diphenyl-1-picrylhydrazyl and nitric oxide scavenging assay. Conclusion: The findings prove that the decoction of *J. sambac has* extensive hepatoprotection against paracetamol-induced toxicity and can be considered as an alternative therapy in hepatic disorders.

**Keywords:** *Jasminum sambac,* hepatoprotective, paracetamol, decoction, toxicity

## Introduction

The largest substantial organ within the human body is the liver. In addition to being essential for metabolic processes, secretion, immunity, and excretion, it contributes to preserving homeostasis within the body. Consequently, toxins such as chemicals, medicines, heavy metals, bacteria, and viruses commonly target the liver and its hepatocytes [1, 2]. The processes above generate a multitude of free radicals that counteract internal antioxidants, leading to the development of both inflammatory (hepatitis) and non-inflammatory (alcoholic liver disease) liver disorders. Nevertheless, repetitive harm arises when the innate protective mechanisms become overwhelmed [3, 4]. Regrettably, the current pharmaceutical choices available for treating liver problems, such as corticosteroids and immunosuppressants, possess notable drawbacks. Herbal drugs have gained notoriety and appeal in recent years due to their effectiveness, low cost, and few unwanted effects [1]. The Oleaceae family of plant species Jasminum has been employed in conventional medication to treat gastritis, diarrhea, arthritis, hepatitis, and dysmenorrhea [5]. Flower stems, leaf bark and roots contain chemicals related to numerous therapeutic benefits, including antiarthritic, antidiarrheal, antibacterial, hepa-

https://doi.org/10.62347/CREZ6896

toprotective, and antioxidant [6]. *Jasminum-sambac*, a member of the Oleaceae family, is popularly known as jasmine [9]. The phytochemical analysis identified the following compounds: quercitrin, hexadecanoic acid, rutin, β-sitosterol, 9-octadecenoic acid, isoquercitrin, R-limonene, quercitrin-3-dirhamnoglycoside, chlorocoumarin, a coumarin derivative, 1-nonadecene, kaempferol, sitosterol, 2, 3-dihydrobenzofuran, 2,6,10-trimethyl, squalene, pentadecne, 1-heptacosanol, 1-Octadecyne, α-tocopherol-β-d-mannoside, kaempherol-3-rhamnoglycosides, α-amyrin, and Jasmintides [7]. Multiple pharmacological studies have provided proof of this substance's antibacterial, antiweight problems, analgesic, anticancer, antipyretic, antioxidant, antidiabetic, lipid-decreasing, insecticidal, and gastroprotective effects [8]. This look aimed to assess the hepatoprotective outcomes of a warm water decoction of *J. Sambac*.

Paracetamol (PCM) is regularly used for analgesia and pyrexia. PCM is a non-prescription drug that may be without problems distributed for therapeutic use without needing a prescription. PCM is typically known as a stable analgesic and antipyretic drug. Nevertheless, the excessive and unregulated use of this medication might lead to acute or chronic liver damage. The first documented cases of PCM-induced hepatotoxicity appeared in the United States in the mid-1980s. Since then, all evidence has pointed to a rising prevalence of this condition. According to Wang and Xie [9], this medication is among the most common causes of drug-induced hepatotoxicity. Based on estimations, overdose patients experience a mortality rate of 0.4%, resulting in approximately 300 deaths per year in the United States [10]. While ingestions of more than 150 mg/kg of a hazardous substance can lead to liver failure, recent research indicates that even smaller doses of PCM may cause acute liver injury and liver failure [11]. The occurrence of abrupt liver failure in certain patients, even when they have taken recommended doses of PCM, has brought significant attention to the concept of "therapeutic misadventure" [11]. Certain patients may exhibit specific etiologies, such as alterations in PCM metabolism at the molecular and mitochondrial levels. These are now under investigation to elucidate their contributions to this potentially life-threatening condition. This study explored the hepatoprotective potential and possible underlying mechanisms of hepatoprotection using a series of *in silico, in vitro*, and *in vivo* experiments.

## Materials and methods

### *Plant material*

Fresh *J. sambac* leaves were picked from the botanical garden of MIMAS, Multan. It was verified by a seasoned taxonomist from Government Emerson College, Multan. The voucher for the collected sample, identified by the collectors as R.R. Stewart and F.W. Pak with code 549, was stored for future reference.

### *Preparation of hot water decoction*

The plant underwent desiccation in a shaded environment. Before grinding, all unnecessary foreign substances and plant matter were carefully eliminated through hand screening. The pulverized foliage underwent hot water extraction. The decoction was preserved in an airtight glass container [12].

### *Animals*

Rabbits of both sexes, with an average body weight of 1.5 kg, were obtained from the animal housing facility associated with the Department of Life Sciences. The participants were given unrestricted access to tap water and commercially available feed. The temperature remained unchanged at 25°C. The study was conducted in accordance with the protocols outlined by the National Institute of Health [13]. The Institutional Animal Ethics Committee authorized the study under the reference number BOS/10/3/23.

### *Chemical and reagents*

Silymarin was purchased from Taqwa Pharmaceuticals, Ltd. Paracetamol [PCM] from Hamaz Pharmaceuticals. Assay kits for determining AST, ALT, ALP, and CRP were obtained from BioTEST trader. All other chemicals were used of analytical purity.

### *Phytochemical analysis*

The presence of vital phytochemical classes, tannins, anthraquinones, saponins, alkaloids, flavonoids, and glycosides was evaluated in HWDJS using the standard procedure [14].

*HPLC analysis*

A binary solvent incline arrangement was utilized in HPLC with the C-18 column [250 mm, internal diameter], suitable for isolating different constituents in thirty-six minutes. The stream was 0.0008 L/min, and 5 m was film depth at a temperature of 30°C in the oven. Linalool, iso-quercetin, and β-sitosterol were prepared as a reference and purchased from Aldrich (St. Louis, USA). To achieve mg/mL, the reductions were organized with methanol. The retention times of samples were compared to standards. The efficacy of HPLC-separated components was assessed using the separation factor and resolution [15].

*Antioxidant assays*

Antioxidant capacity of HWDJS were calculated using DPPH and NO scavenging assays.

*DPPH assay*

The DPPH was evaluated using the documented procedure. To summarise, several concentrations of HWDJS leaf extract (4 mL) were combined with a DPPH solution. Subsequently, the volume was decreased to 5 mL using methanol. The resulting mixture was then incubated in darkness for over 40 minutes. The spectrophotometer was used to measure the absorbance at a wavelength of 517 nm. The inhibitory percentage was quantified in units for vitamin C alternatives, and the studies were conducted in triplicate [16]. Using the equation 2, DPPH inhibitory potential was calculated.

1% = blank/sample divided by blank × 100 (1)

*NO scavenging assay*

HWDJS was prepared using a 10 mg/mL solution of leaf extract in a mixture of water and methanol. Various quantities of extracts (ranging from 100 to 1,000 µg/mL) were obtained by adding distilled water, with Gallic acid serving as the standard. The solutions were stored at 4 degrees Celsius for the experiments. The Griess reagent was produced afresh for utilization. A solution containing 0.5 mL of sodium nitroprusside with a concentration of 10 mM in phosphate-buffered saline was mixed with 1 mL of each extract concentration (ranging from 100 to 1,000 µg/mL) and left to incubate at a temperature of 25 degrees Celsius for three hours. The test samples were treated with equal volumes of extract and fresh Griess reagent, whereas the control samples were treated with equal volumes of fresh Griess reagent and buffer. The color tubes were filled with the designated quantities of extracts. However, they were devoid of sodium nitroprusside. One hundred fifty liters of the reaction mixture were put on a 96-well plate. The UV-Vis microplate reader (Alibaba, Hangzhou, China) was utilized to measure the absorbance at 546 nm, following the methodology outlined in our previous communication [17, 18]. Inhibition percentages (test and standard) were computed and documented utilizing equation 2.

% inhibition = A-B/A × 100 (2)

*Acute oral dose toxicity*

The acute oral dose toxicity test was conducted following the criteria of the Organisation for Economic Co-operation and Development (OECD)-Test Guideline 423. Rabbits were divided into 3 groups, with 6 animals in each group. An acute dose (2,000, 4,000, and 6,000 mg/kg) of HWDJS was administered through oral gavages. The rabbits have been monitored for 14 days after receiving the treatment to record any signs of exhaustion, tremors, or dying [18].

*Hepatoprotective activity*

The hepatoprotective effectiveness of HWDJS was evaluated using the strategies defined previously [1]. The study used a total of thirty rabbits, divided into six groups, with every group including 5 animals.

Group I, received a 1 mL normal saline orally for 7 days. Group II received a 1 mL normal saline orally for 7 days. Group III [Standard] acquired a dosage of 50 mg/kg of silymarin for 7 days. Group IV groups received dose of HWDJS 100 mg/kg for 7 days. Group V groups received dose of HWDJS 200 mg/kg for 7 days. Group VI groups received dose of HWDJS 300 mg/kg for 7 days.

Except Group I, all other groups were administered PCM [2 g/kg] 24 hours following the ultimate treatment, precisely on the 8th day. After subjecting the rabbits to 24 hours of toxicity induction, blood samples were received from their ear veins, after which they were centrifuged at 3,000 rpm for 10 mins. The serum was separated and used for the evaluation of hepatic biomarkers ALP, AST, CRP, and ALT.

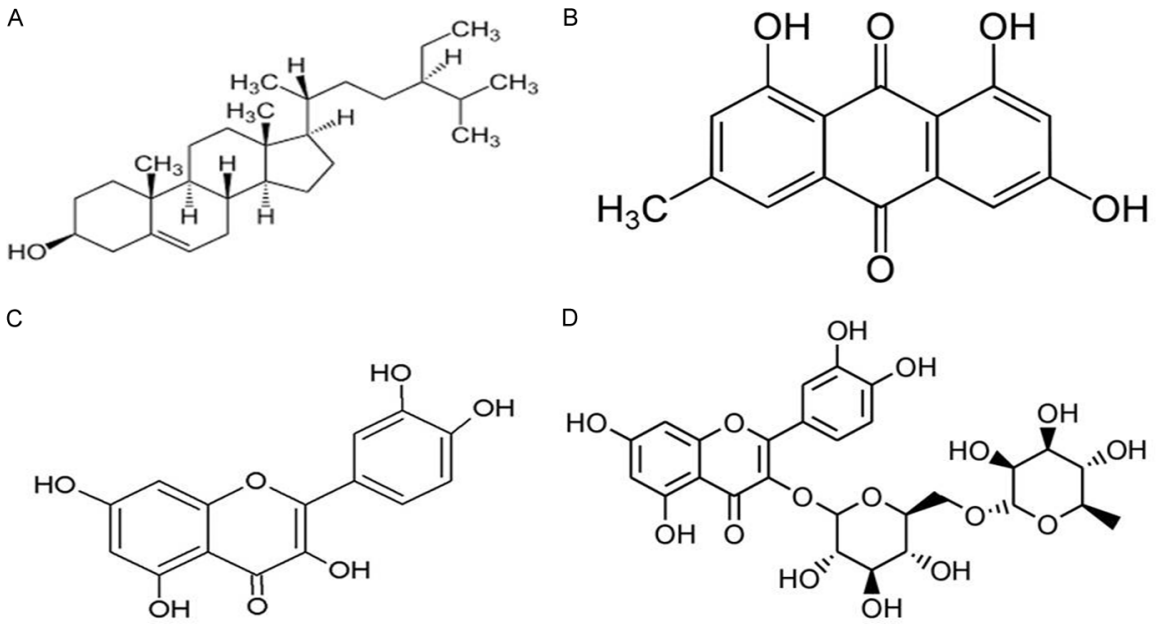


**Figure 1.** Two dimensional structures (2D) of four ligands showing carbon backbone. A: β-sitosterol (CID: 222284). B: Emodin (CID: 3220). C: Quercetin (CID: 5280343). D: Rutin (CID: 5280805).

*Effect on organ weight to body weight ratio*

Liver to body weight ratio was used to assess hepatic damage, necroses and perfusion in all 4 groups intoxicated with PCM with reference to control [16].

*Histopathology*

Animals were euthanized by injecting ketamine, the livers of all rabbits were eliminated to observe the impact of various doses of HWDJS for liver damage because of PCM. The liver tissues were soaked in 10% buffered formalin, and then thin slices [5 μm] were made and embedded them in paraffin and stained with hematoxylin-eosin [19].

*Evaluation of GSH, MDA, and SOD in liver homogenate*

Hepatic samples were homogenized using a 0.05 M sodium phosphate buffer solution after being rinsed with a 7.0 pH ice-cold saline. The homogenate was subjected to ten-minute centrifugation at 4,000 rpm and a temperature of 4°C. Supernatant technique was employed to quantify oxidative pressure signs, which incorporates Superoxide Dismutase (SOD), Malondialdehyde (MDA), and Glutathione (GSH) [1].

*In silico docking study*

*Protein and ligand guidance:* In this study, we acquired the structures of hepato-proteins from the RCSB Protein Data Bank (PDB), a primary facts center within the United States accountable for managing the worldwide Protein Data Bank. The PDB archive is a precious aid containing crucial 3-D shape statistics for significant organic molecules, which include proteins, DNA, and RNA [20]. It mainly looks at applied crystal protein systems BCL-2 (PDB ID: 1G5M) and Human PPAR delta (PDB ID: 2ZNP) downloaded from the PDB database. The protein systems and further purification are completed through the PyMOL Molecular Graphics System (Version 2.5.Zero). The molecular docking analyses were accomplished using PyRx - Python Prescription Zero-Nine. 2, incorporating the Autodock 4.2 software program for digital drug screening. Additionally, docking experiments were performed with the use of Vina 1.1.2.

Ligand structures, essential for molecular docking studies, were acquired from the PubChem database. Four ligands of interest were Quercetin (CID: 5280343), Rutin (CID: 5280805), B-sitosterol (CID: 222284), and Emodin (CID: 3220) (**Figure 1**). To ensure compatibility with

the docking software program, the ligand structures in the Simplified Molecular Input Line Entry System (SMILES) layout have been converted from Structure Data File (SDF) to Protein Data Bank (PDB) format the usage of Obabel 2.4.1. To facilitate the virtual screening system with the use of iGemdock v2.1, the SDF documents were transformed into MOL2 files using Open Babel. Additionally, for docking on AutoDockVina, the compounds have been prepared by changing them into PDB documents using Pymol.

*Virtual screening using iGEMDOCK v2.1:* The docking observation for quercetin (CID: 5280343), Rutin (CID: 5280805), β-sitosterol (CID: 222284), and emodin (CID: 3220) and its interactions with BCL-2 (PDB ID: 1G5M) and Human PPAR delta (PDB ID: 2ZNP) proteins changed into conducted using iGemdock v2.1. IGEMDOCK (Graphical Environment for Recognizing Pharmacological Interactions and Virtual Screening). It serves as a precious device in drug discovery by helping with the identification of lead compounds and know-how of the mechanisms of ligand binding for healing goals [21]. Using iGemdock, every compound inside the library underwent docking into the binding website. The software then analyzed the protein-compound interaction and clustering. The compounds for the post-screening study were selected based on their hydrogen bonding (H), electrostatic (E), and Van der Waal's (V) interaction characteristics. The iGemdock inferred pharmacological interactions based totally on compound structures. Finally, the software ranked and visualized the screening compounds by integrating pharmacological interactions and power-primarily based scoring functions, presenting a comprehensive know-how of the interactions and aiding within the assessment of potential candidates. We implemented the "accurate docking" protocol in our study, using default parameters (Population size of 800, 80 generations, and 10 solutions) for the docking process.

*Pre-molecular docking procedures, active site prediction, and molecular docking:* The molecular docking process was conducted using AutoDock Vina. In the initial steps, water molecules and the standard ligand were removed from the system. Subsequently, hydrogen atoms and charges were added using the Discovery Studio visualization tool and AutoDock tools. To facilitate the docking procedure, the PDB format of the macromolecules and the studied compounds were converted to AutoDock's PDBQT format.

The advanced capabilities of Discovery Studio 2021 were harnessed to predict the active pocket regions of the proteins. This provided valuable insights into the macromolecule's active site, where the pre-loaded ligand binds. The small molecule docking was then focused on this specified binding site, taking into account the total number of rotatable bonds in the ligands. The grid for the docking was defined based on the predicted binding site of the protein structure, with the configuration of x/y/z coordinates set to center_x=31.8028, center_y=18.4151, center_z= 109.2664 in X, Y, Z dimensions. The grid box size was set to size_x=130.260385069, size_y=88.280815-4481, and size_z=225.934748638. This grid configuration was chosen to ensure a targeted and accurate docking analysis within the active site of the protein. Interactions like Hydrogen Bonding and other non-bonded terms between the docked compounds and the protein are displayed and analyzed using Discovery Studio Visualizer.

*Statistical analysis*

Results were analyzed using GraphPad Prism version 8.4.2 software. Mean ± SD was calculated for the quantitative data, paired t-test was used to compare the means of each group before and after applying gels, and one-way analysis of variance (ANOVA) was used to relate the mean of four independent groups using SPSS-23. The confidence interval was 95%, with $P < 0.05$ considered significant.

## Results

*Phytochemical assessment*

Phytochemical evaluation of aqueous methanolic leaf extract of *J.* sambac showed the presence of major phytochemical classes saponins, phenols, coumarins, flavonoids, alkaloids, anthraquinones, and tannins.

*HPLC analysis*

The existence of several phytoconstituents was confirmed using HPLC analysis. Among these, the most significant phytoconstituents,

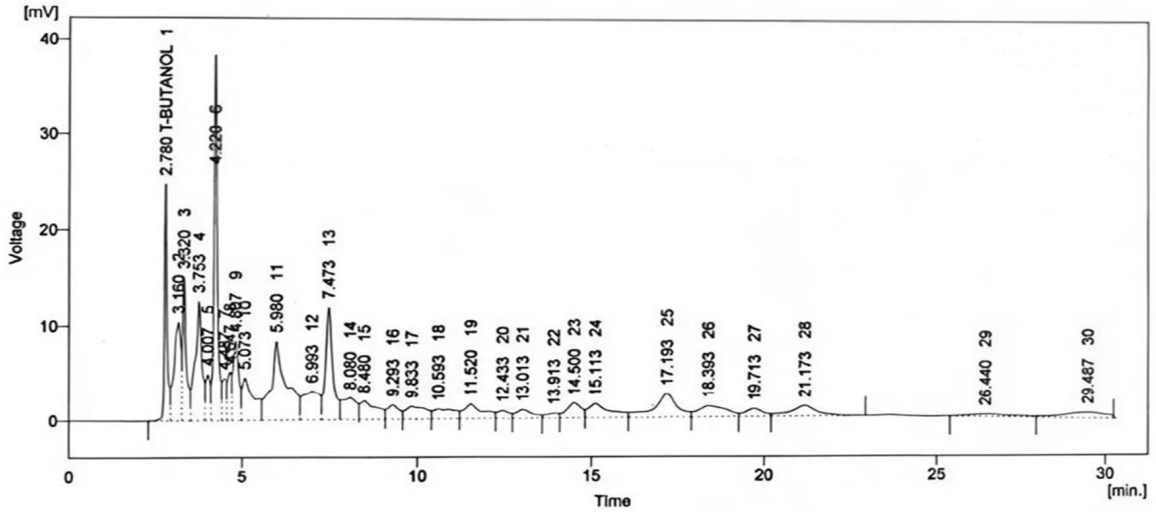


**Figure 2.** HPLC Chromatogram showing the presence of various phytoconstituents; rutin, quercetin, linalool, iso-quercetin, β-sitosterol, iso-quercetin, and β-sitosterol were identified in reference to their retention time.

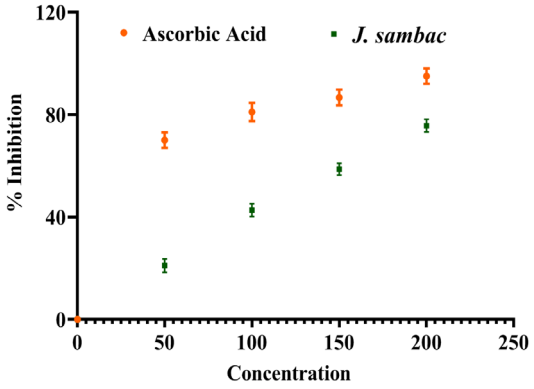


**Figure 3.** Antioxidant potential of HWDJS, referenced to % inhibition of DPPH concerning ascorbic acid.

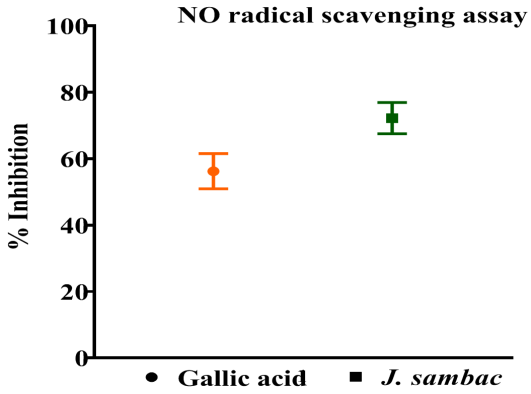


**Figure 4.** Antioxidant potential of HWDJS reference to % inhibition of NO radical scavenging concerning gallic acid.

rutin, quercetin, emodin, rutin, quercetin, linalool, iso-quercetin, and β-sitosterol were identified in reference to their retention time (**Figure 2**).

*Antioxidant assay*

Antioxidant activity of HWDJS recorded using DPPH and NO scavenging assays.

*DPPH assay*

DPPH assay of HWDJS exhibited significant antioxidant activity at a 200 µg/mL concentration of approximately ascorbic acid (**Figure 3**).

*NO scavenging assay*

HWDJS shown the antioxidant activity in NO scavenging assay concentration dependent increase in antioxidant activity was noticed at 77.2%, the highest free radical scavenging activity in comparison with standard gallic acid, as shown in (**Figure 4**).

*Acute oral dose toxicity*

Animals exhibited no notable alterations in behavior when administered a solitary dosage of HWDJS at a dose of 6,000 mg/kg. No instances of lethargy or death were seen in any of the groups.

*Hepatoprotective potential*

The findings of the HWDJS study on the effects of PCM-induced liver damage are presented in **Figure 5**. The intoxicated group was evaluated for significant liver damage by measuring

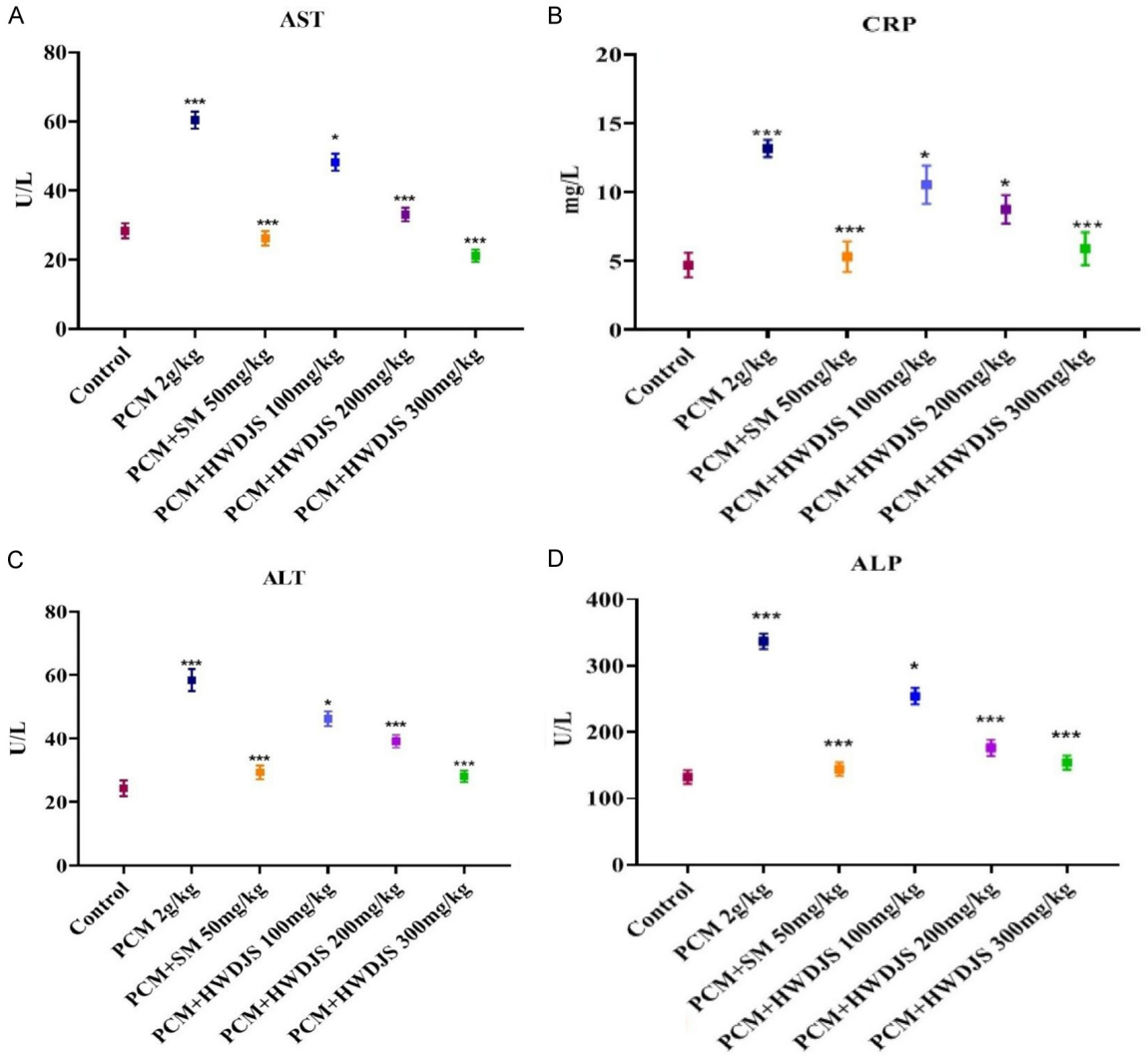


**Figure 5.** Dose-dependent hepatoprotective effect of HWDJS referenced to hepatic markers, AST (A), CRP (B) ALT (C), ALP (D), against PCM intoxication. $*P < 0.05$, and $***P < 0.001$ when compared to the PCM-induced toxicity group using one-way ANOVA following Dunnett's multiple comparison test.

increased serum levels of AST, CRP, ALT, and ALP, which showed a dose-dependent relationship with the control group.

*Organ weight to body weight ratio*

PCM significantly elevated the ratio compared to the standard. Three groups who received HWDJS have a liver-to-body weight ratio lower than the group that was dosed with PCM (**Figure 6**).

*Histopathology*

The liver histology showed changes associated with the control group that received conventional therapy. Conversely, the administration of PCM by itself led to the intoxication of rabbits. In comparison to the control group, it caused significant changes in the structure of the liver, including necrosis, ballooning degeneration, and inflammation. The histopathologic annotations support the findings of the biochemical analysis (**Figure 7**).

*Effect on antioxidant measurements*

The antioxidant levels in rabbits with toxicity induced by PCM and the treated groups are presented in **Table 1**. Rabbits exposed to PCM-induced toxicity exhibited significantly elevated levels of MDA, which is indicative of oxidative damage and the primary cause of peroxidized

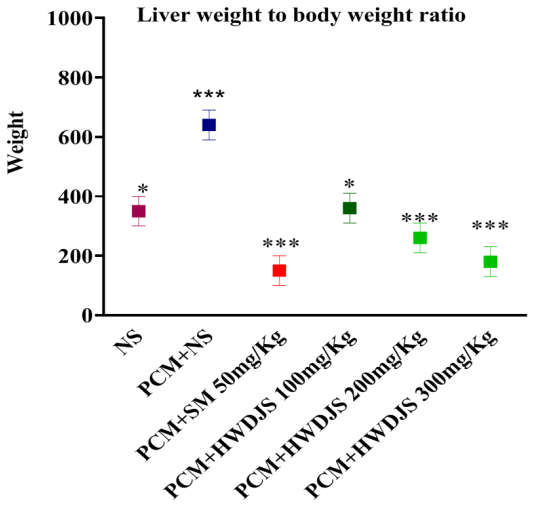


**Figure 6.** Dose dependent hepatoprotective effect of HWDJS referenced to liver to body weight ratios in control and PCM-induced-toxicity group. *$P < 0.05$, and ***$P < 0.001$ when compared to PCM-induced toxicity group using one-way ANOVA following Dunnett's multiple comparison test.

polyunsaturated fatty acids in comparison to the control group. HWDJS treatment effectively mitigated the liver against PCM-induced toxicity. In addition, it was noted that the treatment of HWDJS led to a significant increase in the antioxidant level, as indicated by the higher levels of glutathione and superoxide dismutase in contrast to the group that was exposed to induced toxicity (**Table 1**).

*Molecular docking*

This study selected two hepatic proteins: B-cell lymphoma 2 (BCL-2; PDB ID: 1G5M), which inhibits apoptosis by preventing cytochrome c release from mitochondria, and Peroxisome proliferator-activated receptors [PPAR delta; PDB ID: 2ZNP], which regulates lipid metabolism and energy homeostasis, particularly through fatty acid oxidation with their interaction. The molecular docking studies with quercetin, rutin, β-sitosterol, and emodin can provide valuable insights into their interactions with BCL-2 and PPAR delta, informing the development of healing dealers concentrated on apoptosis and lipid metabolism-associated pathways.

*BCL-2 (PDB ID: 1G5M) docking*

Regarding the docking of BCL-2 (PDB ID: 1G5M), β-sitosterol exhibited the best binding energy (-five.29), indicating a strong interaction and capability as a BCL-2 inhibitor for apoptosis regulation in sicknesses like most cancers. Emodin additionally showed considerable binding electricity (-four.4), suggesting favorable inhibitory houses in opposition to BCL-2. Quercetin displayed slight binding electricity (-four.25), indicating an inexpensive affinity and capability for modulating BCL-2 activity. Rutin verified the lowest binding power (-2.92), suggesting weaker inhibitory results as compared to different compounds examined, albeit none the less showing a few affinity for BCL-2. These findings suggest β-sitosterol, emodin, and quercetin as promising candidates for further investigation in apoptosis-associated therapeutics targeting BCL-2 (**Figure 8**; **Table 2**).

*PPAR delta (PDB ID: 2ZNP) docking*

In the docking, note that PPAR delta (PDB ID: 2ZNP), β-sitosterol displayed the highest binding energy (-5.81), indicating a strong interplay and suggesting its capability to modulate PPAR delta's lipid metabolism-regulating capabilities. Emodin showed widespread binding power (-4.40), suggesting a positive interaction with PPAR delta and a potential effect on lipid metabolism pathways. Quercetin exhibited moderate binding energy (-3.84), indicating an affordable affinity for PPAR delta and its ability to contribute to its consequences on lipid metabolism and associated disorders. However, rutin demonstrated the lowest binding electricity (-0.89), suggesting a weaker interaction and potentially restricted effect on PPAR delta pastime than other compounds tested (**Table 2**). These findings offer insight into the ability roles of these compounds in modulating PPAR delta characteristics and lipid metabolism.

In summary, the docking outcomes recommend that β-sitosterol and emodin display sturdy interactions with BCL-2 and PPAR delta, indicating their potential as twin-targeting dealers for apoptosis law and lipid metabolism modulation. Quercetin demonstrates reasonable affinities for both proteins, while rutin indicates weaker interactions, particularly with PPAR delta. These findings offer valuable insights into the potential healing roles of those compounds in illnesses related to apoptosis dysregulation and metabolic problems.

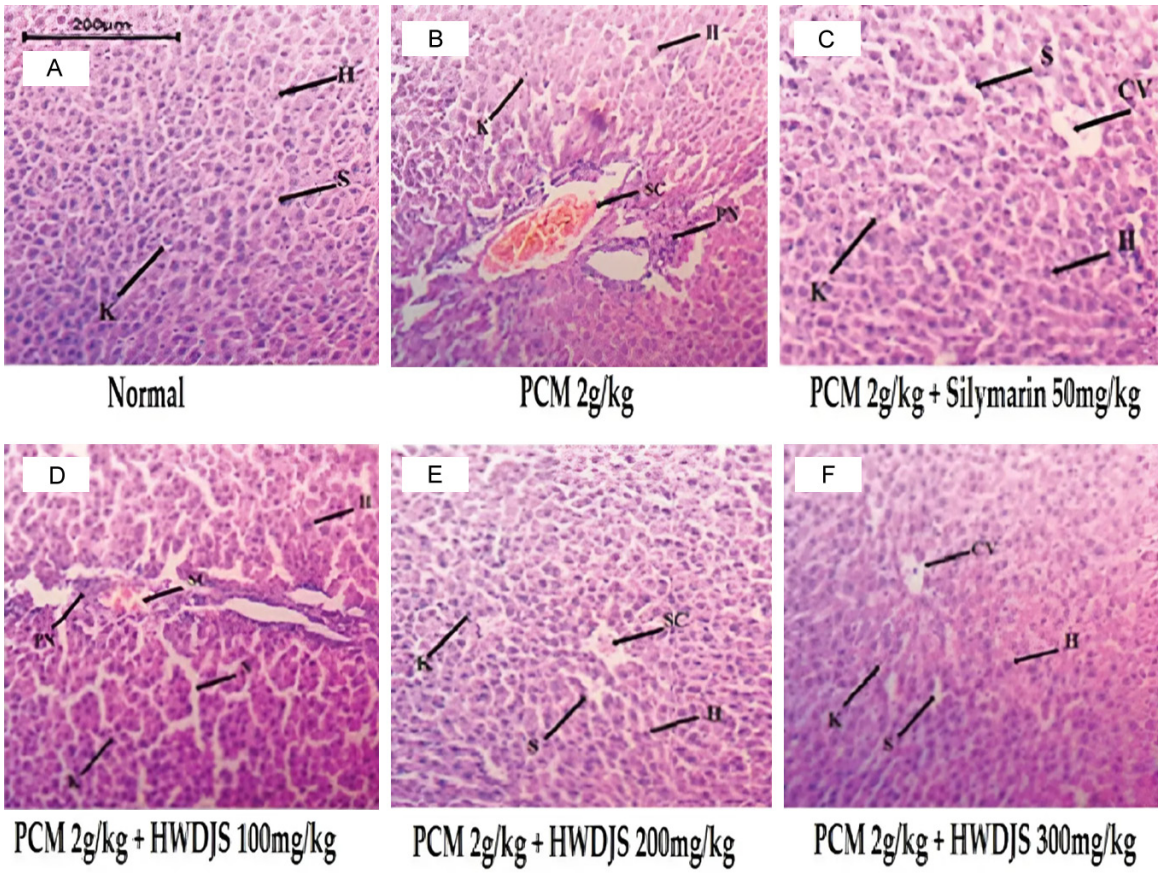


**Figure 7.** A photomicrograph illustrates the histopathologic changes in the liver of rabbits caused by PCM-induced toxicity and the subsequent prevention achieved through the use of HWDJS leaves. The liver sections were examined using hematoxylin and eosin staining at a magnification of ×100. Kupffer cells are denoted as K, the central vein as CV, hepatocytes as H, piecemeal necrosis as PC, sinusoids as S, and sinusoidal congestion as SC.

**Table 1.** Hepatoprotective effect of HWDJS leaf on MDA, GSH, and SOD

| Group | MDA (nmole/mg of Protein) | GSH (nmole/mg of Protein) | SOD (unit/mg of Protein) |
|---|---|---|---|
| Control | 0.43±0.01 | 17.57±0.58 | 9.25±0.24 |
| Paracetamol (2 g/kg) | 1.70±0.02# | 5.87±0.27# | 3.17±0.30# |
| Silymarin (50 mg/kg) | 0.81±0.01*** | 12.48±0.78*** | 7.05±0.30*** |
| HWDJS (100 mg/kg) | 1.56±0.01** | 7.70±0.15** | 4.05±0.26** |
| HWDJS (200 mg/kg) | 1.54±0.01** | 7.91±0.43** | 5.01±0.19** |
| HWDJS (300 mg/kg) | 1.52±0.01*** | 9.24±0.16*** | 5.36±0.38*** |

**: significant, ***: highly significant, ns: non significant, #: toxicity.

*Predicted binding websites of ligands*

In the molecular docking we examined BCL-2 (PDB ID: 1G5M) and PPAR delta (PDB ID: 2ZNP) with four ligands (β-sitosterol, emodin, quercetin, and rutin), designated analysis of the interacting residues sheds mild at the binding patterns and potential modes of movement of these compounds. For BCL-2, β-sitosterol exhibited the highest binding strength, forming interactions with amino acids, which include VAL A:148, LEU A:97, and PHE A:151, suggesting a robust interplay and ability as a BCL-2 inhibitor. Emodin, quercetin, and rutin also displayed various levels of affinity, interacting with amino acids, which include MET A:16, LYS A:17, and GLU A:13, indicating their capacity roles in modulating BCL-2 activity. Similarly, in PPAR

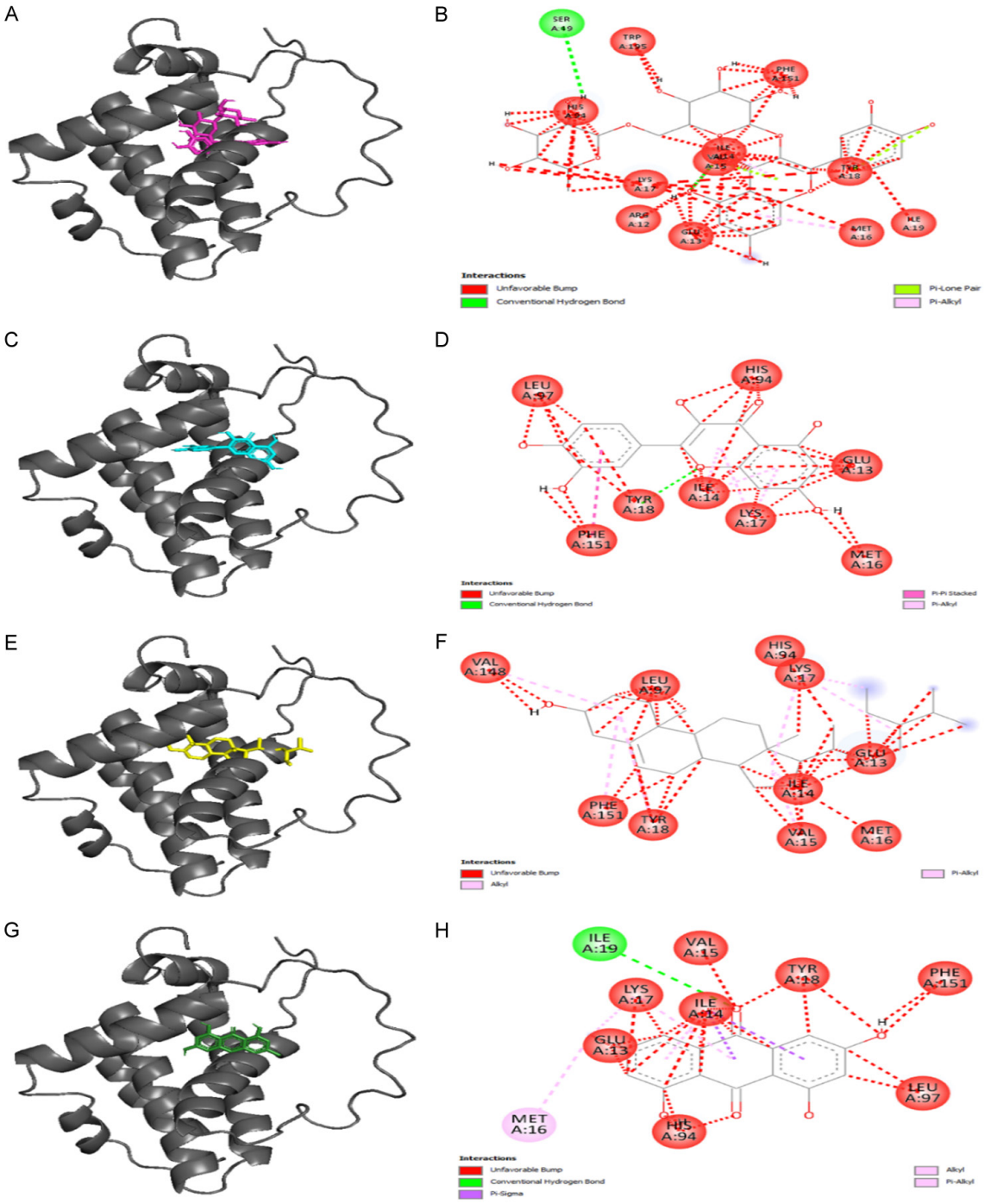


**Figure 8.** Three-dimensional (3D) representations of docked complexes formed between BCL-2 (1G5M) and ligands. (A and B) depict the 3D docked complex of rutin with 1G5M, (C and D) show the complex of quercetin with 1G5M, (E and F) display the complex of β-sitosterol with 1G5M, and (G) illustrates the complex of emodin with 1G5M. Additionally, (B, F, and H) provide two-dimensional (2D) diagrams highlighting interacting residues of the protein and ligand in front of their respective 3D structures.

delta docking, B-sitosterol, and emodin confirmed interactions with LEU A:211, indicating localized binding websites and capacity modulation of lipid metabolism-regulating features. Quercetin's interaction with PPAR delta was not specified in the provided data, while rutin displayed a similar binding pattern to B-sitosterol and emodin, indicating potential interactions

**Table 2.** Binding energies of β-sitosterol, emodin, quercetin, and rutin with BCL-2 (PDB ID: 1G5M) and PPAR delta (PDB ID: 2ZNP)

| Protein_Ligand | Binding Energy |
|---|---|
| BCL-2 (1g5m)::B-sitosterol | -5.29 |
| BCL-2 (1g5m)::Emodin | -4.4 |
| BCL-2 (1g5m)::Quercetin | -4.25 |
| BCL-2 (1g5m)::Rutin | -2.92 |
| PPAR delta (2znp)::B-sitosterol | -5.81 |
| PPAR delta (2znp)::Emodin | -4.42 |
| PPAR delta (2znp)::Quercetin | -3.84 |
| PPAR delta (2znp)::Rutin | -0.89 |

BCL-2: B-cell leukemia/lymphoma 2 protein, PPAR delta: Peroxisome proliferator-activated receptor delta.

with LEU A:211 (**Tables 2**, **3**). These findings provide valuable insight into the specific amino acids involved in ligand-protein interactions, enhancing our understanding of their therapeutic implications in apoptosis regulation and lipid metabolism modulation.

## Discussion

The preliminary findings of the acute toxicity study conducted on experimental rabbits using HWDJS indicated the absence of any harmful outcomes, such as mortality or sickness, at all tested doses, including 6,000 mg/kg. PCM is an analgesic and antipyretic medication that does not contain steroids. PCM is metabolized primarily through sulfotransferase (SULT) and UDP-glucuronosyltransferase (UGT) enzymes at therapeutic levels [22]. This metabolism produces non-toxic compounds removed from the body through urine [23]. Only a minuscule proportion of the urine remains unchanged. The cytochrome P-450 enzyme CYP-2E1 primarily catalyzes the highly reactive intermediate N-acetyl-p-benzoquinone imine (NAPQI), which is how the residual PCM undergoes metabolism [24]. When combined with glutathione (GSH), NAPQI is often swiftly neutralized [25]. Excessive PCM consumption results in an overdose that increases the activity of phase II metabolizing enzymes, causing a reduction in GSH levels and an elevation in NAPQI [22].

Consequently, cellular proteins, particularly those found in mitochondria, get bonded to a covalent sulfhydryl group. Huang et al. [26] observed this phenomenon in a study. Hepatocyte death occurs, leading to oxidative stress and impaired mitochondrial functioning [24].

The histologic examination of liver cells demonstrated that pre-treatment with HWDJS preserved the integrity of the nuclear envelope, preventing its damage induced by PCM toxicity (**Figure 6**). The liver function test (AST, CRP, ALT, and ALP) is crucial for identifying hepatoprotection. In contrast to the intoxicated group, HWDJS had a dose-dependent ($P < 0.05$-$0.00$) positive effect in reducing hepatic markers (**Figure 4**). Reports indicate that the hepatoprotective benefits of plants can be ascribed to their substantial quantities of flavonoids. Phytochemical analysis shows that the HWDJS possesses a significant abundance of flavonoids (**Figure 2**). Thus, flavonoids will likely affect the potential hepatoprotection of HWDJS in rabbits. The current study showed that using HWDJS led to a noteworthy drop in CRP levels in the groups who were given the extracts. The discovered effect can be ascribed to the antioxidant characteristics of HWDJS (**Figure 4**), which may be the result of its phytoconstituents flavonoid or vitamin C, as confirmed with the aid of prior research on its antioxidant efficacy [14]. HWDJS showed good antioxidant potential during DPPH and NO scavenging assays (**Figures 2**, **3**). This antioxidant potential of HWDJS provides another logical ground for believing its hepatoprotective potential. Prior research has hypothesized that saponins can decrease the levels of LPO byproducts [1, 24]. The quantity of this effect is believed to be influenced by way of the dosage of saponins provided [13]. The outcomes of this experiment were uploaded to the modern-day body of data that helps preceding research on the hepatoprotective results of saponins [27]. The phytochemical analysis HWDJS found an extensive presence of saponins as evidence.

Excessive intake of PCM was reported to lower the GSHt/GSSG ratio and boost the MDA number. The cited outcomes are mentioned as signs of lipid peroxidation [1]. Herbal treatments include several phytochemicals, including flavonoids, phenols, thiols, and saponins, that have been determined to have hepatoprotective features. These substances can avoid the process of LPO, facilitate the recuperation of broken mobile membranes, shield against mitochondrial harm, and eliminate oxygen-unfastened radicals [27]. The initial evaluation of HWDJS discovered excessive attention to triterpenes, flavonoids, and saponins. These chemicals ought to enhance the liver-defensive

**Table 3.** Interacting residues of β-sitosterol, emodin, quercetin, and rutin with BCL-2 (PDB ID: 1G5M) and PPAR delta (PDB ID: 2ZNP)

| Protein Ligand | Interacting residues of protein |
|---|---|
| BCL-2 (1g5m)::B-sitosterol | VAL A:148, LEU A:97, PHE A:151, TYR A:18, HIS A:94, LYS A:17, VAL A:15, GLU A:13, MET A:16, ILE A:14 |
| BCL-2 (1g5m)::Emodin | MET A:16, ILE A:19, LYS A:17, GLU A:13, VAL A:15, ILE A:14, HIS A:94, TYR A:18, PHE A:151, LEU A:97 |
| BCL-2 (1g5m)::Quercetin | LEU A:97, PHE A:151, TYR A:18, ILE A:14, HIS A 94, LYS A:17, GLU A:13, MET A:16 |
| BCL-2 (1g5m)::Rutin | SER A:49, HIS A:94, TRP A:195, LYS A:17, ARG A:12, GLU A:13, ILE A:14, VAL A:I5, PHE A:151, TER A:18, MET A:16, ILE A:19 |
| PPAR delta (2znp)::B-sitosterol | LEU A:211 |
| PPAR delta (2znp)::Emodin | LEU A:211 |
| PPAR delta (2znp)::Quercetin | _ |
| PPAR delta (2znp)::Rutin | LEU A:211 |

BCL-2: B-cell leukemia/lymphoma 2 protein, PPAR delta: Peroxisome proliferator-activated receptor delta.

outcomes of HWDJS via performing as antioxidants. Research has shown that medicinal flora can lessen damage to hepatocytes, endothelial cells, vascular smooth muscle, and monocytes, demonstrating its hepatoprotective character [19].

KATP channel activation has verified hepatoprotective properties in cardiomyocytes and enhances the discharge of atrial natriuretic peptide. Likewise, activating KATP channels in hepatocytes has been proven to have protective benefits for the liver and enhance the release of atrial natriuretic peptides. The activation of KATP channels has been linked to apoptosis, hypertrophy, oxidative stress, inhibition of hepatic inflammation, and extended manufacturing of endothelial nitric oxide synthase [29].

The use of HWDJS grows located to decrease the production of MDA, a byproduct formed at a few degrees inside the oxidation of cell membranes. GSH and SOD enzymes act as antioxidants by facilitating the conversion of radical anion superoxide into $O_2$ and $H_2O_2$ [24, 28, 30]. This study concluded that HWDJS introduced an increase in the degrees of GSH and SOD in rabbits that dealt with PCM (**Table 1**).

Studies have documented the effects of crude extracts, remoted chemical materials, and solvent fractions from the Jasminum genus on liver diseases. *J. Grandiflorum* extracts have been shown to mitigate hepatotoxicity prompted by CCl4 toxicity through inhibition of oxidative pressure [31].

PPARs, activated by endogenous ligands, including fatty acids and analogous compounds, govern vital metabolic processes in the liver and other organs. They comprise a family of ligand-dependent transcription factors. There are currently three identified isoforms of PPARs: PPARα, PPARβ/δ, and PPARγ. Each isoform possesses distinct characteristics regarding its agonist specificity, distribution, and ability to regulate mammalian lipid metabolism and energy homeostasis [32, 33]. Because all alterations that transpire during liver damage perturb metabolic functionality, worsen liver damage, and render PPARs crucial therapeutic targets for treating these conditions.

In addition to alcoholic liver disease, the most alarming liver diseases on a global scale include metabolic-associated fatty liver disease, fibrosis, hepatocellular carcinoma, and hepatitis A, B, and C infections. Several of them are significant contributors to global mortality. Consequently, it is critical to comprehend the function of PPARs as metabolic regulators in the progression of these pathologies and to develop novel ligands that effectively modulate the activity of these receptors while minimizing adverse effects. Considering these facts, various phytoconstituents of HWDJS were examined and found to be significant in regulating PPARs' varying affinities (**Tables 2**, **3** and **Figure 9**). Similarly, hepatocyte BCL2 is one of the primary indicators of hepatic injury in the early stages of the disease. Mitochondrial dysfunction and lipid peroxidation are the major contributory factors. Various phytoconstituents of HWDJS were examined and found to be sig-

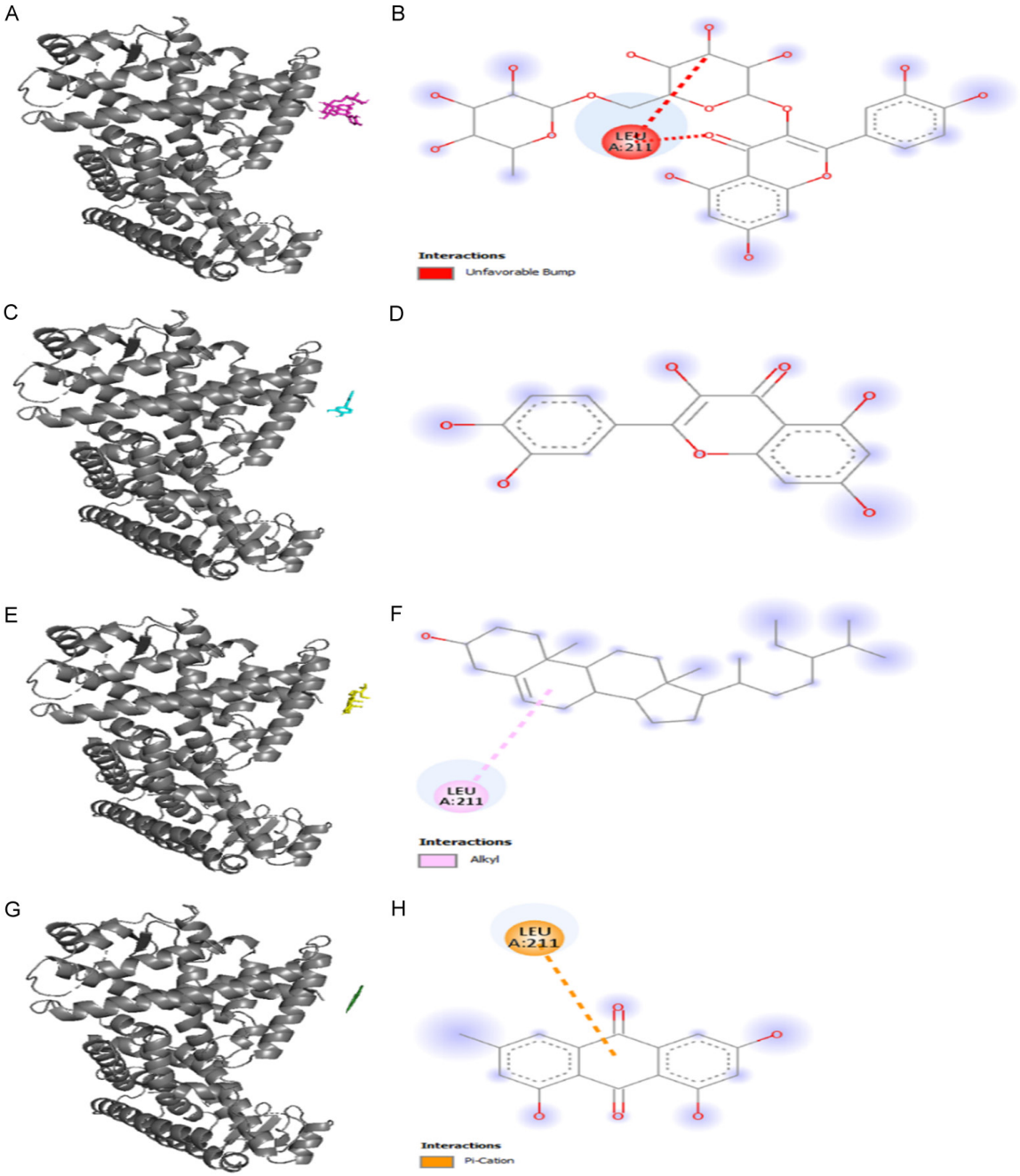


**Figure 9.** Three-dimensional representations of docked complexes formed between PPAR delta (2ZNP) and ligands. (A, C, and E) depict the 3D docked complexes of rutin, quercetin, and β-sitosterol with 2ZNP, respectively, while (G) illustrates the complex of emodin with 2ZNP. Additionally, (B, D, F, and H) provide 2D-diagrams highlighting interacting residues of the protein and ligand in front of their respective 3D.

nificant in regulating PPARs' varying affinities (**Tables 2**, **3** and **Figure 8**).

Based on the results of this research, HWDJS has hepatoprotective properties against PCM-induced toxicity in rabbits. Further research is required to comprehensively analyze the molecular factors contributing to HWDJS's antioxidant potential and ascertain its likely mechanism.

## Conclusion

The research offers initial scientific validation for the therapeutic advantages of HWDJS in hepatic tissues. The management of HWDJS

resulted in the prevention of plasma AST, CRP, ALT, and ALP outcomes, in addition to a decrease in hepatic antioxidant enzymes together with GSH, SOD, and MDA. These findings suggest that HWDJS correctly blanketed the liver from damage. The hepatoprotective efficacy of HWDJS towards PCM-induced liver damage is attributed, as a minimum component, to its vast antioxidative interest as tested in DPPH and NO assays. The histopathology observation implies that the HWDJS-dealt-with groups exhibited a decrease in cell damage in comparison to the PCM intoxicated. The findings of this study provide proof to warrant additional research on HWDJS as an herbal hepatoprotective agent.

## Acknowledgements

This work was funded by the Researchers Supporting Project number (RSP2025R376), King Saud University, Riyadh, Saudi Arabia.

## Disclosure of conflict of interest

None.

## Abbreviations

ALP, global burden of disease; ALT, activities of daily living; CRP, Western Ontario and McMaster Universities Arthritis Index; AST, numeric pain rating scale; NSAIDs, nonsteroidal anti-inflammatory drugs; HPLC, cyclooxygenase 2; IL, interleukin; NF-κB, nuclear factor-κB; TNF-α, tumor necrosis factor-α; DPPH, 2,2-diphenylpicrylhydrazyl; NO, nitric oxide; SOD, superoxide dismutase; WHO, World Health Organization; WMA, World Medical Association; ROS, reactive oxygen species; TLR-4, Toll-like receptor-4; TGF-β1, Transforming growth factor-β1; PGE-2, prostaglandin E-2; MAPK, mitogen-activated protein kinase; GSH, fourier transform infrared spectroscopy; HPLC, high performance liquid chromatography; NO, inducible nitric oxide synthase; PGN, peptidoglycan; LPS, lipopolysaccharides.

**Address correspondence to:** Dr. Imran Ahmad Khan, Department of Pharmacy, MNS University of Agriculture, Multan 60000, Punjab, Pakistan. E-mail: imran.ahmad@mnsua.edu.pk; Dr. Sabiha Fatima, Department of Clinical Laboratory Science, College of Applied Medical Sciences, King Saud University, Riyad, Saudi Arabia. E-mail: sabmehdi@ksu.edu.sa

## References

[1] Rathore FA, Attique R and Asmaa Y. Prevalence and perceptions of musculoskeletal disorders among hospital nurses in Pakistan: a cross-sectional survey. Cureus 2017; 9: e1001.

[2] Irfan M, Qurat-Ul-Ain, Iqbal MO, Chen J, Khan MK, Sattar M and Khan IA. Association between anthropometric measurements of chairs and biomechanical variables leading to musculoskeletal problems in students at different government universities of Multan. Am J Transl Res 2023; 15: 6136-6147.

[3] Williams A, Kamper SJ, Wiggers JH, O'Brien KM, Lee H, Wolfenden L, Yoong SL, Robson E, McAuley JH, Hartvigsen J and Williams CM. Musculoskeletal conditions may increase the risk of chronic disease: a systematic review and meta-analysis of cohort studies. BMC Med 2018; 16: 167.

[4] Cieza A, Causey K, Kamenov K, Hanson SW, Chatterji S and Vos T. Global estimates of the need for rehabilitation based on the Global Burden of Disease study 2019: a systematic analysis for the Global Burden of Disease Study 2019. Lancet 2021; 396: 2006-2017.

[5] Ain QU, Khan IA, Raza MA, Anjum A, Khan MK, Perwasha P and Ishaq S. Evaluation of polyherbal gel for musculoskeletal injuries in industrial workers. Work 2024; 78: 447-460.

[6] Iqbal MO, Naeem M, Mumtaz A, Ahmed MM, Ahmad A, Riaz R, Mesbah Z and Munawar N. Biochemical evaluation and medicinal ability of Jatropha mollissima in hepatic disorders. Am J Transl Res 2022; 14: 7178-7188.

[7] Iqbal MO, Manzoor M, Mumtaz A, Riaz R, Arshad S, Khan IA, Javaid U, Manzoor Z, Munawar SH, Andleeb S, Ahmed MM and Aslam A. Evaluation of the hepatoprotective activity of hydroalcoholic extract of Alhagi camelorum against valproic acid-induced hepatotoxicity in rats. Biomed Pharmacother 2022; 150: 112953.

[8] Iqbal MO and Yahya EB. In vivo assessment of reversing aminoglycoside antibiotics nephrotoxicity using Jatropha mollissima crude extract. Tissue Cell 2021; 72: 101525.

[9] Omer Iqbal M, Bashir Yahya E, Andleeb S, Masood Ahmed M, Umar Javaid M, Shakeel W and Iqbal I. In vivo assessment of reversing cisplatin-induced nephrotoxicity using Jatropha mollissima crude extract and its potential cytotoxicity. Saudi J Biol Sci 2021; 28: 7373-7378.

[10] Iqbal MO, Ahmed MM, Arshad S, Javaid U, Khan IA, Manzoor M, Andleeb S, Riaz R, Munawar SH, Manzoor Z and Mumtaz A. Nephroprotective effects of Alhagi camelorum against cisplatin-induced nephrotoxicity in albino wistar rats. Molecules 2022; 27: 941.

[11] Wade AG, Crawford GM, Young D, Corson S and Brown C. Comparison of diclofenac gel, ibuprofen gel, and ibuprofen gel with levomenthol for the topical treatment of pain associated with musculoskeletal injuries. J Int Med Res 2019; 47: 4454-4468.
[12] Veloso C, Cardoso C and Vitorino C. Topical fixed-dose combinations: a way of progress for pain management? J Pharm Sci 2021; 110: 3345-3361.
[13] Byl NN. The use of ultrasound as an enhancer for transcutaneous drug delivery: phonophoresis. Phys Ther 1995; 75: 539-553.
[14] Khan IA, Janbaz KH and Saqib F. Antidiarrheal activity of methanolic leaf extract of Rumex vesicarius. Bangladesh J Pharmacol 2016; 11: 175-180.
[15] Ain QU, Abid MUH, Hashim M, Ishaq S, Manzoor A, Perwasha P, Mizgan GE, Iqbal MO, Munawar SH, Manzoor Z and Khan IA. Anticoagulant and thrombolytic activities of leaf extract of mangifera indica in smokers. Tob Regul Sci 2022; 1189-1201.
[16] Ain QU, Iqbal MO, Khan IA, Bano N, Naeem M, Jamaludin MI, and Devaraj S. Phytochemical, antioxidant, antipyretic, and anti-inflammatory activities of aqueous-methanolic leaf extract of Mangifera indica. Am J Transl Res 2023; 15: 4533-4543.
[17] Mizgan GE, Kousar S, Khan IA, Perwasha P, Gul H, Aslam I, Abbas A and Ul-Ain U. Evaluation of anti-clotting and thrombolytic potential of the aqueous-methanolic extract of Jasminum sambac. Pak J Pharm Sci 2022; 35: 1747-1754.
[18] Kunhachan P, Banchonglikitkul C, Kajsongkram T, Khayungarnnawee A and Leelamanit W. Chemical composition, toxicity and vasodilatation effect of the flowers extract of Jasminum sambac (L.) Ait."G. Duke of Tuscany". Evid Based Complement Alternat Med 2012; 2012: 471312.
[19] Al-Snafi AE. Pharmacological and therapeutic effects of Jasminum sambac-a review. Indo Am J Pharm Sci 2018; 5: 1766-1778.
[20] Belango YMC, Cruz AF, Miguel RB, Rotairo CRL and Oli RAT. Anti-inflammatory property of the formulated topical gel from the crude leaf extracts of Sampaguita (Jasminum sambac L. family: Oleaceae). Int J Chem Eng Appl 2016; 7: 199.
[21] Khan IA, Hussain M, Munawar SH, Iqbal MO, Arshad S, Manzoor A, Shah MA, Abbas K, Shakeel W and Syed SK. Jasminum sambac: a potential candidate for drug development to cure cardiovascular ailments. Molecules 2021; 26: 5664.
[22] Khan IA, Lodhi AH, Munawar SH, Manzoor A, Manzoor Z and Raza MA. Formulation and evaluation of rutin-allicin gel against diabetic foot ulcer. Lat Am J Pharm 2020; 39: 725-729.
[23] Khan IA, Aziz A, Sattar M, Munawar SH, Manzoor Z, Raza MA, Fatima G and Hannan A. Evaluation of wound healing potential of Rumex vesicarius L. Leaf extract and fractions in rabbit. Afr J Tradit Complement Altern Med 2015; 12: 60-64.
[24] Khan IA, Aziz A, Manzoor Z, Munawar SH, Sarwar HS, Afzal A and Raza MA. Study on antipyretic activity of Rumex vesicarius leaves extract in albino rabbits. Vet World 2014; 7.
[25] Aziz A, Saqib F, Khan IA, Ashraf MM, Ashraf MN and Raza MA. Dermatological evaluation of anti-irritant and anti-inflammatory effect of plumerin-r isolated from the latex of plumeria rubra linn. Lat Am J Pharm 2018; 37: 317-20.
[26] Rafique R, Khan ZU, Akram MAN, Javid K, Iltaf S, Shaukat M, Shaukat H and Ali S. Phytochemical analysis of stem and leaf extracts of Jasminum sambac (L.) Aiton by FTIR method: analysis of stem and leaf of Jasminum sambac (L.). Biol Sci-PJSIR 2023; 66: 199-204.
[27] Khan IA, Hussain M, Syed SK, Saadullah M, Alqahtani AM, Alqahtani T, Aldahish AA, Asiri S and Zeng LH. Pharmacological justification for the medicinal use of Plumeria rubra Linn. in cardiovascular disorders. Molecules 2021; 27: 251.
[28] Iqbal MO, Khan IA, Manzoor A, Arshad S, Sial AS, Dar E and Shaikh AR. Cardioprotective effect of hydroalcoholic leaf extract of Jatropha mollissima on isoproterenol-induced myocardial infarction in rats. Pharmacogn Mag 2021; 17: 251-256.
[29] Khan IA, Hussain M, Hussain N, Alqahtani AM and Alqahtani T. Cardioprotective Effect of Rumex vesicarius Linn. Leaf extract against catecholamine-induced cardiotoxicity. Molecules 2022; 27: 3383.
[30] Zhang L, Liang X, Wang B, Lin Z, Ye M, Ma R, Zheng M, Xiang H and Xu P. Six herbs essential oils suppressing inflammatory responses via inhibiting COX-2/TNF-α/IL-6/NF-κB activation. Microchem J 2020; 156: 104769.
[31] Huang H, Yang X, Li W, Han Q, Xu Z, Xia W, Wu M and Zhang W. Structural characterization and immunomodulatory activity of an arabinogalactan from Jasminum sambac (L.) Aiton tea processing waste. Int J Biol Macromol 2023; 235: 123816.
[32] Ceccacci S, Lucia A, Tortora A, Colantuono A, Carotenuto G, Tito A and Monti MC. Jasminum sambac cell extract as antioxidant booster against skin aging. Antioxidants (Basel) 2022; 11: 2409.
[33] Alvarez AM, DeOcesano-Pereira C, Teixeira C and Moreira V. IL-1β and TNF-α modulation of proliferated and committed myoblasts: IL-6 and COX-2-derived prostaglandins as key actors in the mechanisms involved. Cells 2020; 9: 2005.